Journal of Applied Polymer Science

Processing and Characterization of Injection Moldable Polymer–Particle Composites Applicable in Brazing Processes

Stefan Kirchberg,[1] Ulrich Holländer,[2] Kai Möhwald,[2] Gerhard Ziegmann,[1] Friedrich-Wilhelm Bach[2]

[1]Institute of Polymer Materials and Plastics Engineering, Faculty of Natural and Materials Sciences, Clausthal University of Technology, Agricolastr. 6, 38678 Clausthal-Zellerfeld, Germany

[2]Institute of Materials Science, Faculty of Mechanical Engineering, Leibniz University Hannover, An der Universität 2, 30823 Garbsen, Germany

Correspondence to: S. Kirchberg (E-mail: stefan.kirchberg@tu-clausthal.de)

ABSTRACT: A novel method has been developed to process highly filled polymer–particle composites to test samples as braze metal preforms. Polypropylene (PP), low-density polyethylene (LD-PE) and high-density polyethylene (HD-PE) were used as polymer matrices. Two types of nickel-based braze metal microparticles (Ni 102 and EXP 152) were compounded to the polymer matrices at filler contents up to 65 vol %. With enhancing filler content, torque at kneading rotors, and injection molding parameter were significantly affected by increasing viscosity. Injection molded composites show well-distributed spherical microparticles and particle–particle interactions. Polymers decompose residue-free at temperatures above 550°C, even for their composites. Adding particles reduces polymer crystallinity, whereas defined cooling at 5°C/min significantly increases the crystallinity and melt peak temperature of polymers compared to undefined cooling prior injection molding. Storage modulus of polymers increases significantly by adding filler particles. LD-PE + 65 vol % EXP 152 show the most suitable composite performance. © 2012 Wiley Periodicals, Inc. J. Appl. Polym. Sci. 129: 1669–1677, 2013

KEYWORDS: composites; applications; degradation; thermogravimetric analysis (TGA); differential scanning calorimetry (DSC)

Received 15 August 2012; accepted 20 November 2012; published online 18 December 2012
DOI: 10.1002/app.38862

INTRODUCTION

Composites based on thermoplastic matrices and functionalized micro- and nanoparticles are used for numerous applications regarding the functional properties and the content of filler particles, as well as the properties of polymer matrices.[1–5] The main advantage of polymer–particle composites is the easy and cost-efficient process ability in kneading, extrusion and injection molding processes at filler contents up to 70 vol %.[6] Therefore, complex geometrical parts with custom-made properties can be produced to substitute cost-intensive applications.[7,8]

Many components are manufactured by means of brazing technology.[9] Whenever high demands on corrosion and heat resistance of the components are required, preferably stainless steel combined with nickel-based brazes are used.[10,11] In principle different kinds of techniques can be applied for brazing stainless steel, e.g., induction brazing and furnace brazing in vacuum or protective gases. Generally, processing this kind of material is a demanding task, which requires a careful control of all parameters for a successful brazing process.[12] In this context, a precise deposition of the filler metal at the joint plays a central role for accurate brazing results. Nickel-based braze metals are supplied usually as powders due to its metallurgy. The braze powder has to be fixed in some way to enable a deposition onto the components to be brazed. At present this is done by preparing pastes from the powders using aqueous or organic solutions with certain amounts of dissolved organic binders. The deposited pastes must be dried accurately, as the solvents can disturb the following brazing process. This demands cost- and time-consuming process steps. Furthermore, there are many complex devices like heat exchangers, where inner joints must be brazed. An accurate deposition of brazing pastes before assembling the components to be brazed is difficult in this case. Brazing defects resulting from removing the deposited paste due to assembling the parts is a severe problem for the processing of such devices, because the dried pastes show poor form stability and insufficient adhesion to the metal surfaces.

Combining thermoplastic polymers and braze metal powder in polymer-particle composites offer new possibilities for the application of powdered braze metals. The solvent-free composites can be used to produce tailored made preforms for both simple and complex joint geometries. The preforms show high form stability and can be precisely positioned at the joint when assembling the components to be brazed. Furthermore, braze metal preforms

Applied Polymer SCIENCE

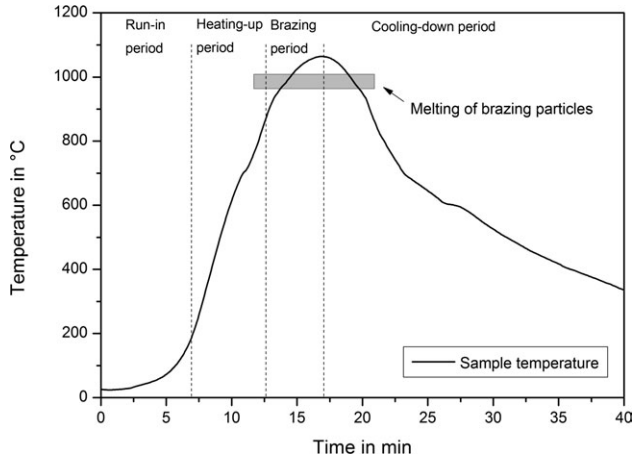

Figure 1. Temperature profile of a brazing process in a conveyor belt furnace processing stainless steel with the nickel-based filler metal Ni 102.

can be produced in mass-production by injection molding process even at complex geometric structure.

In contrast to other applications of polymeric composites, special demands have to be made on polymer bonded braze powder preforms, e.g., residue-free decomposition of the polymer during heating-up period in brazing process (see Figure 1). In fact, temperatures well below the melting temperature of the braze and oxygen-free process conditions are preferred, since the brazing processes are performed in inert or reducing atmospheres (argon, nitrogen, and hydrogen).[13–15] The amount of polymeric binder should be as low as possible, in order to minimize a spread of the braze powder during melting and decomposition of the polymer matrix during the brazing process. On the other hand, a certain content of polymer is necessary for a successful injection molding process. Hence, the evaluation of the usability in brazing processes requires the identification of appropriate polymer–particle composites. Therefore, the effect of braze particles on the thermal degradation and the structure of the polymer matrices as well as on the dynamic mechanical properties of the composites has to be analyzed. Compounding, injection molding and thermal analysis of polymer–particle composites applicable in brazing processes are not reported in literature up to now.

MATERIALS AND METHODS

Three technical semi-crystalline thermoplastic polymers were used as polymeric matrices: polypropylene (PPH 754 32 RNA, Dow Costumer Information Group, Edegem, Belgium), low-density polyethylene (LD-PE, Lupolen 1806 H, LyondellBasell, Ludwigshafen, Germany) and high-density polyethylene (HD-PE, Hostalen GC 7260, LyondellBasell, Ludwigshafen, Germany) with specific density of 0.9 g/cm^3, 0.919 g/cm^3 and 0.96 g/cm^3, respectively.

Two types of conventional braze metal powders—Ni 102 (WLM 3007.2 Ni 102, Womet GmbH, Willich, Germany) and EXP 152 (EXP 152, Womet GmbH, Willich, Germany)—with particle size up to 106 μm and melting temperature of about 1000°C were used. The specific densities of the gas atomized Ni 102 and EXP 152 microparticles are 7.97 g/cm^3 and 7.77 g/cm^3, respectively.

Particle size distribution of braze metal powders was analyzed in a water-based dispersion by High-Resolution Laser Diffraction (HRLD) using a laser diffractometer (Analysette MicroTec plus, Fritsch GmbH, Idar-Oberstein, Germany).

Thermoplastics and preheated braze metal microparticles were compounded for 10 min at 200°C and 50 rpm in a corotating lab kneader (PolyLab Rheomix 600p, ThermoHaake, Thermo Fisher Scientific, Karlsruhe, Germany). The composites were granulated and further injection molded to test specimen (30 × 10 × 4 mm^3) using a hydraulic injection molding machine (Arburg Allrounder 220S, Arburg, Lossburg, Germany).

Viscosity measurements were performed at 200°C by a high pressure capillary rheometer (Rheograph75, Goettfert Werkstoff-Pruefmaschinen GmbH, Germany). The force transducer resolution accuracy is 0.04%. The adaptive resolution of the pressure sensors is given as ±0.005%.

The shape and distribution of the braze metal microparticles in the injection-molded composite samples are characterized and energy dispersive X-ray spectroscopy (EDX) was performed using a scanning electron microscope (CamScan 4, Cambridge Scanning, Cambridge, UK).

The particle filler fraction and decomposition behavior of the polymer matrix were analyzed using a thermogravimetric analyzer (TGA Q5000IR, TA Instruments, Alzenau, Germany). TGA was performed starting from ambient temperature (≈30°C) to 800°C in high-resolution mode (10/4/4) with modulated heating rate of 10°C/min, sensitivity of 4, and resolution of 4. Typical temperature profile in a continuous working protective gas furnace for a brazing process (see Figure 1) was used as well. The balance measurement resolution accuracy is 0.1%. For temperature calibration the well-known Curie temperature of a nickel standard sample was measured as a reference.

The volume percent ζ_F of the examined polymer–particle composites can be calculated from the specific density of filler material ρ_F and polymer matrix ρ_M as well as the weight percent of the polymer matrix w_P in the composite (see eq. 1).

$$\varsigma_F = \frac{1}{\left(1 + \frac{\rho_F}{\rho_M} \cdot \frac{w_P}{1-w_P}\right)} \cdot 100\% \qquad (1)$$

The weight percentage of the polymer matrix can be calculated from the filler weight percentage w_B, measured by TGA at temperatures exceeding the degradation temperature of the polymer.

The temperature-dependent changes in polymer structure were determined using a differential scanning calorimeter (DSC Q2000, TA Instruments, Alzenau, Germany) in temperature range from 0 to 200°C at a heating/cooling rate of 5°C/min under nitrogen atmosphere. For temperature calibration the melt temperature of indium, lead, tin, and zinc standards have been measured to achieve a minimum temperature deviation of 0.2°C.

Semi-crystalline thermoplastic polymers are characterized by temperature-dependent melting and crystallization of the crystalline polymer structure. Measuring heat flow in DSC allows calculating the melting enthalpy ΔH_m (area within melting peak in heat flow) and the melt peak temperature of polymers T_m regarding to

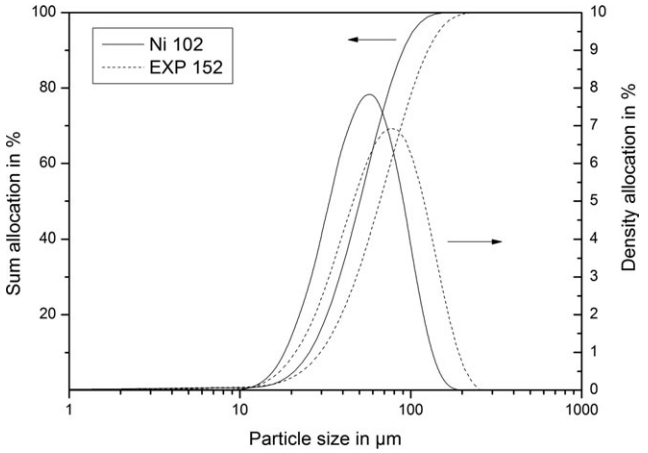

Figure 2. Sum and density allocation of nickel-based powders Ni 102 and EXP 152.

their filler content. Crystallinity K of semi-crystalline polymers can be calculated using melting enthalpy of 100% crystalline polymer (ΔH_m^0), which is given in Ehrenstein et al. as 209 J/g and 293 J/g for PP and (LD-/HD-)PE, respectively (see eq. 2).[17]

$$K = \frac{\Delta H_m}{\Delta H_m^0} \cdot 100\% \tag{2}$$

A dynamic mechanical thermal analyzer (DMTA) (DMA Q800, TA Instruments, Alzenau, Germany) in forced vibration single cantilever mode is used for mechanical characterization. The temperature ranges from 40 to 150°C at a heating rate of 3°C/min and an induced frequency of 8 Hz. An amplitude of 5 μm (equal to a maximum strain of $\varepsilon \sim 1.4 \times 10^{-4}$) is applied for a standard experiment. The temperature has been calibrated using indium, lead, tin, and zinc standards to achieve a minimum temperature deviation of 0.2°C. The resolution of the loss factor ($\tan \delta = E''/E'$) is 1×10^{-4}, which is the ratio of the loss modulus E'' to the storage modulus E'. The repeating accuracy of storage modulus is 3%.

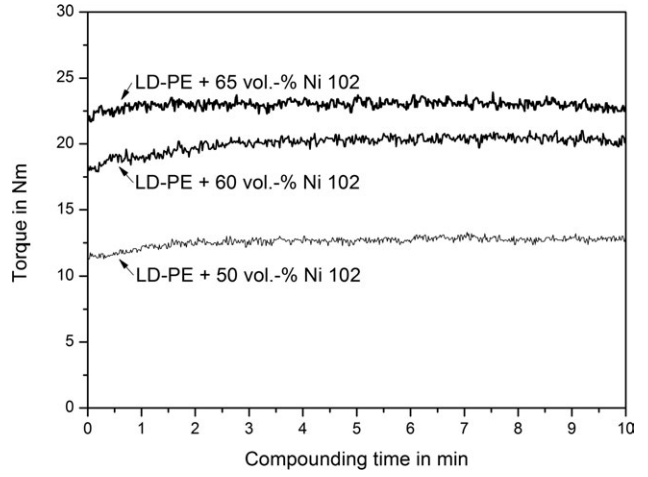

Figure 3. Time-dependent torque at the roller rotors of LD-PE + Ni 102 composites at filler content of 50, 60, and 65 vol % (200°C, 50 rpm).

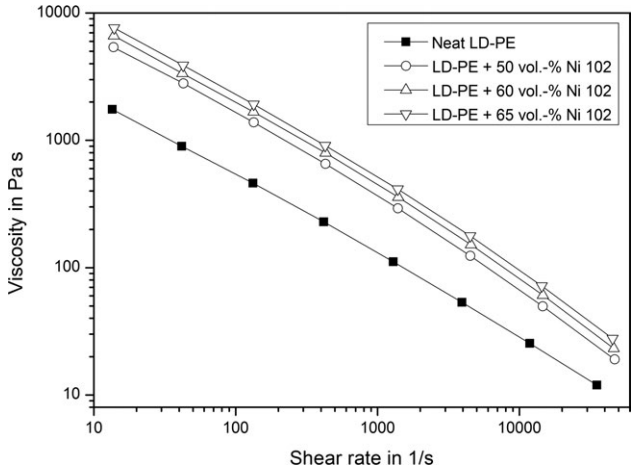

Figure 4. Viscosity graphs of neat LD-PE and LD-PE + Ni 102 composites at filler content of 50, 60, and 65 vol % (200°C).

RESULTS AND DISCUSSION

Figure 2 shows the mono-modal particle size distribution of the two nickel-based powders in comparison. EXP 152 particles show with $d_{50} = 73$ μm a slightly higher mean particle size compared to Ni 102 particles with $d_{50} = 56$ μm. Sum allocation and density allocation of EXP 152 particles are shifted to higher particle size, correspondingly.

The nickel-based microparticles were compounded to the polymer matrix at filler content of 50, 60, and 65 vol % using a corotating lab kneader. Figure 3 shows the torque at the corotating roller rotors while compounding LD-PE + Ni 102 composites.

To reduce the temperature gradient to the polymer melt, the particles were preheated up to 100°C before compounding. Compounding time starts when the whole amount of the particles is mixed into the polymer matrix. The torque at the roller rotors increases with filler content from 12.5 to 22.5 Nm. The slightly increase in torque at compounding time up to 2 min is caused by the inhomogeneous distribution of the particles in polymer matrix. At compounding time exceeding 2 min no further significant change in torque can be detected. Consistent

Table I. Injection Molding Parameter of Neat PP, LD-PE, HD-PE (0 vol %) and Their Polymer–Particle Composites

	0 vol %	50 vol %	60 vol %	65 vol %
Melt temperature in °C	200	200	200	200
Flow rate in cm^3/s	22	22	22	22
Injection pressure in bar	500	1000	1500	2500
Packing pressure in bar	400	800	1200	2000
Mold temperature in °C	30	80	80	80

Applied Polymer SCIENCE

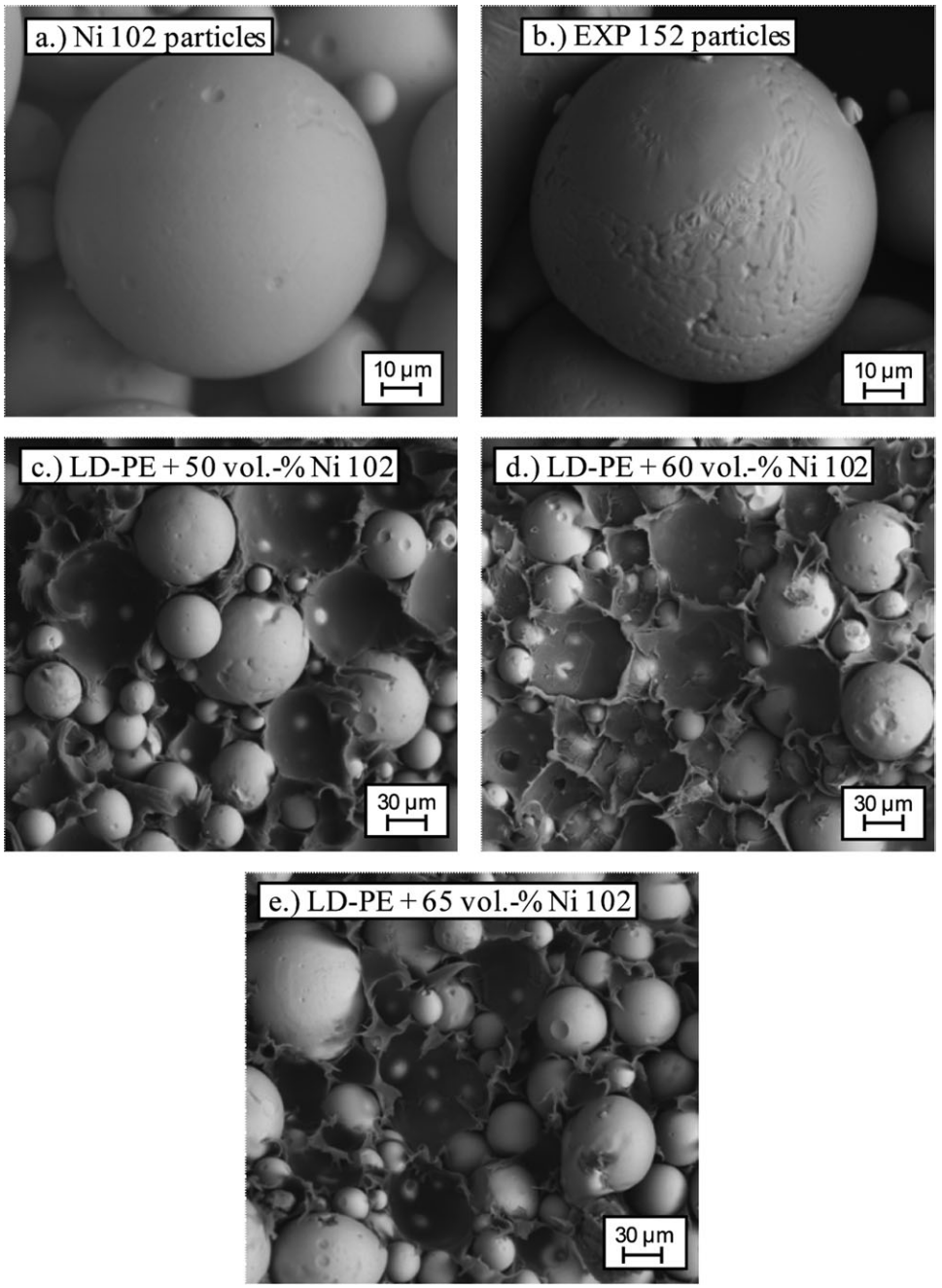

Figure 5. (a,b) Ni 102- and EXP 152 particles and (c–e) fracture surface of injection molded LD-PE + Ni 102 composite parts (back scattering SEM, magnification (a, b): ×1000, (c–e): ×300).

torque with minor changes indicates homogeneously distribution of the particles in the polymer matrix.

Increase of torque in compounding process is affected by the increase of viscosity by adding rigid particles to the polymer melt. Figure 4 illustrates results of viscosity measurements on LD-PE + Ni 102 composites at process-specific temperature (200 °C) and shear rate range (13 up to 47.000 1/s). Viscosity increases with filler content, affecting the torque in kneading process (see Figure 3). However, adding particles to the polymer melt does not influence the shape of the viscosity graphs. Viscosity is affected by polymer material and volume fraction of braze particles but not significantly altered by the braze particle material for all examined composites (not shown). Besides torque in kneading process, injection molding parameters are also affected by viscosity.

Injection molding was performed using the parameter listed in Table I. Packing pressure was fixed at 80% of injection pressure. Neat polymer materials (PP, LD-PE, HD-PE) were processed as reference at relatively low injection pressure and mold temperature because of the low viscosity and consequently relatively

Table II. Results of Element Analysis (in wt %) from EDX on Ni 102- and EXP 152 Particles as well as at the Surface of the White Spots of LD-PE + 50 vol % Ni 102 [in Figure 5(c)] and LD-PE + 50 vol % EXP 152 Composites

	Ni 102 particle	LD-PE + 50 vol % Ni 102	EXP 152 particle	LD-PE + 50 vol % EXP 152
Ni	81.54	81.67	60.74	60.81
Fe	3.93	3.65	0.05	0.04
Cr	8.42	8.22	33.69	33.58
Si	6.12	6.46	5.52	5.57

high flow ability of neat polymer melts. Injection pressure increases with filler content from 500 bar (at 0 vol %) to the system-dependent maximum pressure of 2500 bar (at 65 vol %). This is caused by increasing viscosity and thermal conductivity, which decreases flow ability of composite melts. Flow ability was slightly improved by raising mold temperature up to 80°C to reduce temperature gradient between polymer melt and mold. However, it was not possible to produce samples based on PP and HD-PE with filler content of 65 vol %.

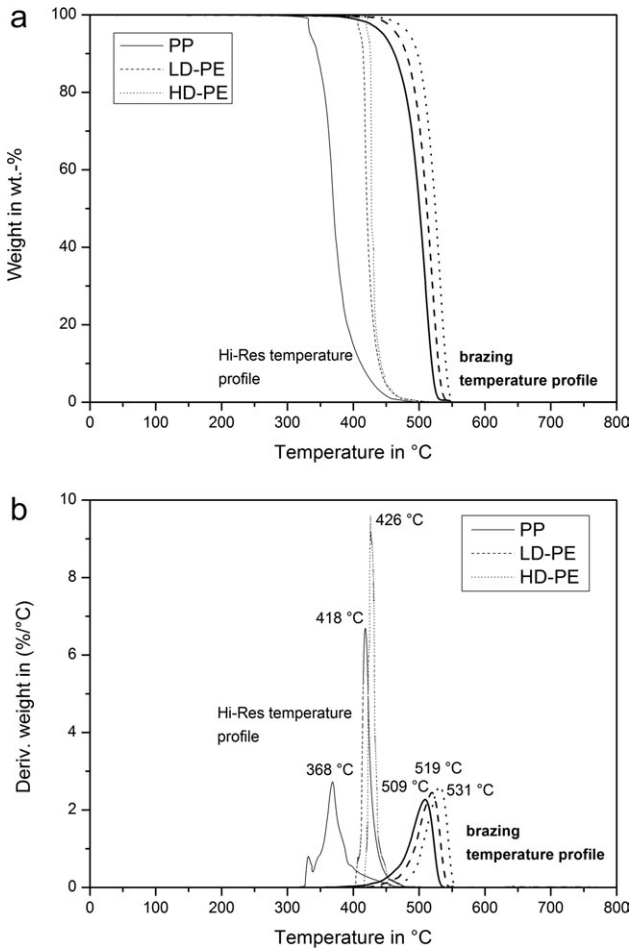

Figure 6. (a) Thermal degradation and decomposition residue of polymer materials and (b) inflection point temperature of polymer degradation depending on temperature profile.

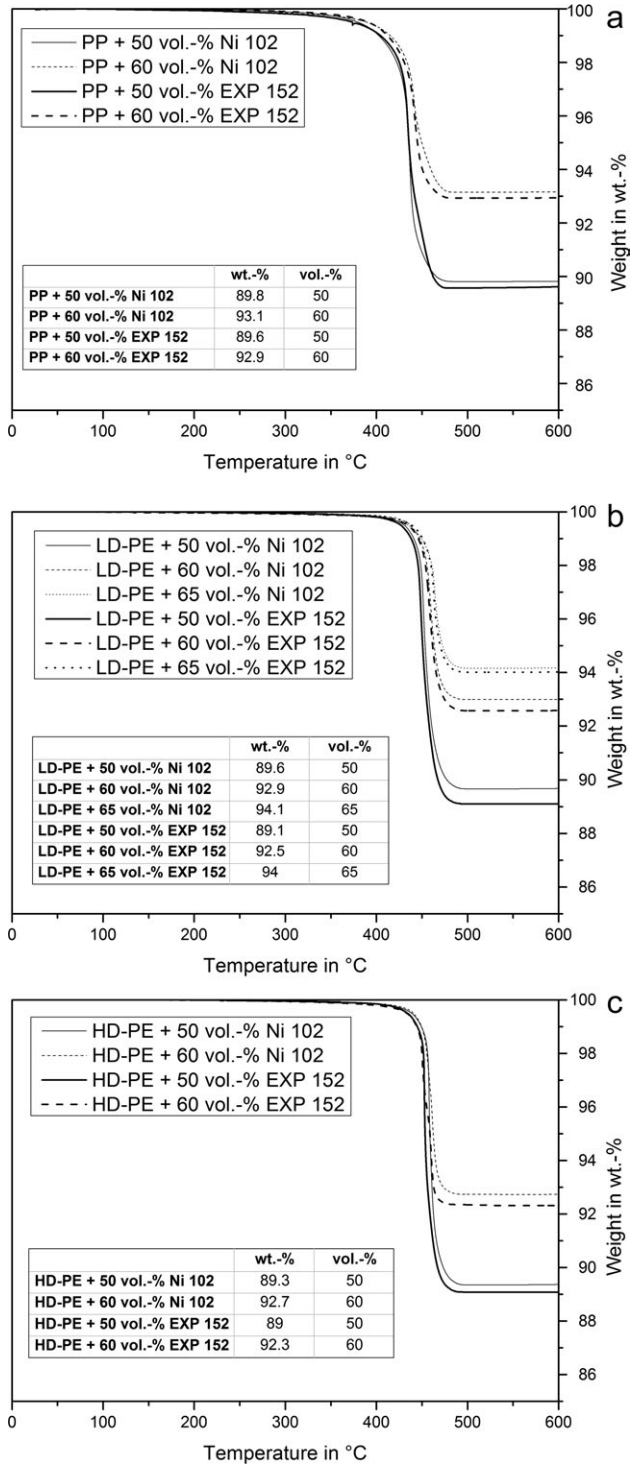

Figure 7. Thermogravimetric analyses on polymer–particle composites to determine thermal degradation behavior and filler content.

SEM micrographs in Figure 5(a,b) illustrate the spherical shape of Ni 102 and EXP 152 particles, whereas several EXP 152 particles have irregular rod-like shape (not shown) and wrinkled

Applied Polymer SCIENCE

Table III. DSC Results from Heat-(Cool)-Heat Measurement

	First heating		Second heating	
	K[a](%)	T_m (°C)	K[a](%)	T_m (°C)
PP	46	168	54	165
PP + 50 vol % Ni 102	45	165	53	160
PP + 60 vol % Ni 102	45	163	50	158
PP + 50 vol % EXP 152	46	165	48	159
PP + 60 vol % EXP 152	39	162	48	157
LD-PE	31	110	33	109
LD-PE + 50 vol % Ni 102	30	107	32	107
LD-PE + 60 vol % Ni 102	28	108	31	108
LD-PE + 65 vol % Ni 102	29	104	33	106
LD-PE + 50 vol % EXP 152	31	108	30	107
LD-PE + 60 vol % EXP 152	30	107	32	107
LD-PE + 65 vol % EXP 152	29	107	28	107
HD-PE	65	133	76	132
HD-PE + 50 vol % Ni 102	60	131	70	132
HD-PE + 60 vol % Ni 102	63	130	73	132
HD-PE + 50 vol % EXP 152	63	131	73	131
HD-PE + 60 vol % EXP 152	63	129	72	130

Crystallinity K and melt peak temperature T_m.
[a]Calculated from eq. (2) and melting enthalpy ΔH_m measured in DSC.

surfaces caused by the production process. The fracture surfaces of the injection molded composite parts show homogeneously distributed microparticles embedded in the polymer matrix, exemplarily shown in Figure 5(c–e) for LD-PE + Ni 102 composites. Several particles are broken out of the matrix described by roll marks on the fracture surface.

On the surface of these roll marks white spots can be detected, which are caused by particles situated behind the polymer matrix and verified by energy dispersive X-ray spectroscopy (EDX, Table II). The element analysis in Table II shows similar weight content of nickel (Ni), iron (Fe), chrome (Cr), and silicon (Si) of Ni 102- and EXP 152 particles in comparison to the surface of the white spots of their composites, respectively.

The frequency of particle–particle contact [number of white spots in Figure 5(c–e)] increases with filler content and describes the interparticulate interaction in the composites. Similar results were found in literature for PP + FeSi composites with filler content up to 70 vol %.[16]

Thermograms obtained on injection molded test specimens in thermogravimetric analysis (TGA) are shown in Figure 6. Figure 6(a) shows the degradation behavior of neat polymers in temperature range from ambient temperature to 800°C at high-resolution (Hi-Res) and brazing temperature profile (see Figure 1). The inflection point temperature of the weight loss graphs in Figure 6(a) is defined by the peak temperature of the derivative weight in Figure 6(b). The degradation of the polymer materials starts at a lower temperature for high-resolution temperature profile in comparison to the temperature profile used in brazing process (see Figure 1). High heating rate in temperature profile of brazing process increases temperature inertia and inhomogeneous temperature distribution of the sample, which shifts the inflection point of polymer degradation to higher temperature [see Figure 6(b)]. PP exhibits the lowest temperature stability followed by LD-PE and HD-PE at both temperature profiles. The examined polymer materials decompose residue-free at temperatures above 550°C, whereby the main requirement for the use in brazing processes is fulfilled.

TGA results of the examined composites are shown in Figure 7(a–c) at high-resolution temperature profile. Weight percent w_P of the polymer was calculated by the total weight loss in TGA graphs. Furthermore, weight percent of the particles was determined by the residual weight at temperatures above 550°C. Afterwards, the particle volume percent ζ_F was calculated from the polymer weight percent w_P (see eq. 1). Calculated volume percent (vol %) and measured weight percent (wt %) of braze particles are mentioned in the tables enclosed in Figure 7(a–c). The calculated volume percent of the filler particles agree with the desired filler fraction. All examined polymer–particle composites show comparable degradation behavior and constant weight at temperatures above 500°C.

Melting enthalpy ΔH_m and melt peak temperature T_m of neat polymers and their composites were determined in heat-(cool)-heat mode in DSC. Table III shows crystallinity K, calculated from melting enthalpy using eq. (2), and melt peak temperature at first and second heating. The first heating shows the polymer structure resulting from the conditions while injection molding and subsequently undefined cooling in the mold and at ambient temperature after demolding. The heat flow results obtained in second heating describe change in the polymer structure prior to the defined cooling at 5°C/min in DSC. The results from the enclosed cooling step are not mentioned in Table III.

Neat polymers show slightly higher crystallinity and melt peak temperature compared with their composites, mainly for PP and HD-PE. Crystallinity and melt peak temperature of LD-PE are not significantly affected by filler content and heat cycle. PP, HD-PE, and their composites show a wide range of increased crystallinity up to 11% from first to second heating, whereas LD-PE and its composites are characterized by the lowest increase in crystallinity (up to 4%). Crystallinity of PP varies from 32 to 54%, which is in between that of LD-PE and HD-PE. However, polymer crystallinity of the polymer–particle composites cannot be clearly correlated with filler content in the examined range of braze particle content.

Polymer melts in general show an amorphous structure in molten state. Cooling from molten to solid state changes polymer structure from a disordered amorphous structure to a highly ordered crystalline structure, which causes increased shrinkage and reduces dimensional stability of the polymer material. With increasing filler content of rigid particles the amount of polymer and consequently the shrinkage of the composite material will be reduced. LD-PE and its composites show most suitable form stability caused by the lowest shrinkage as a result of lowest crystallinity of the polymer prior injection molding.

Dynamic mechanical analysis (DMA) was performed to characterize the mechanical behavior of the polymer–particle composites. Figure 8 shows the storage modulus of neat polymers and their polymer–particle composites in a wide temperature range from 30°C up to ~ 145 °C. In comparison, neat LD-PE exhibits the lowest storage modulus values, whereas neat PP and HD-PE present almost equal mechanical performance. Adding particles increases storage modulus up to 15 times (for LD-PE + 65 vol % EXP 152 at 30°C). HD-PE + 60 vol % EXP 152 shows at 30°C a storage modulus of 7600 MPa, which is up to 1.44 times higher than the PP- and LD-PE composites at equal filler content. The general storage modulus of composites containing Ni 102 particles is lower than that of EXP 152 particle-filled composites. According to the literature, the storage modulus decreases with increasing temperature due to the softening of the polymer matrix, whereby the influence of the mechanical properties of the rigid particles becomes smaller.[18] At low temperatures ($T << T_m$), the mechanical properties of the particles are dominant. This is caused by the increase of polymer–particle and particle–particle interactions at the interface of the composite [see Figure 5(c–e)].

The results of debindering tests on rectangular injection molded specimen (30 × 10 × 4 mm^3, shown at the bottom of Figure 9) in continuous furnace at temperature up to 600°C under nitrogen-atmosphere are illustrated in Figure 9. Melting of the polymer matrix in the injection molded test specimen takes place at temperatures between 104 and 168°C (see melt peak temperature T_m in Table III). Polymer melting at temperatures exceeding T_m reduces form stability due to the increasing flow ability of the polymer in the composites. Due to the high melt flow rate (MFR) of the used PP matrix (52 g/10 min, at 230°C, 2.16 kg), PP-based composites show relatively high flow ability and consequently low geometrical stability. In comparison, LD-PE and HD-PE show much lower MFR values of 1.6 g/10 min (190°C, 2.16 kg) and 8.0 g/10 min (190°C, 2.16 kg) and increased form stability. The polymer melting behavior can be correlated with the different spreading of the composite materials in debindering tests. Consequently, LD-PE composites exhibit the most suitable form stability, followed by HD-PE- and PP composites. The examined polymers are decomposed residue-free at maximum temperature of 600°C, which was also shown in TGA (see Figures 6 and 7).

To further improve the form stability of the composite parts, cross-linking of polymer structure will be used in the next modification step provided by electron beam up to 100 kGy output powers. Therefore, PP has to be compounded with a cross-linking additive (BETALINK-Master PP01, Plastic Technology Service Marketing- & Vertriebs-GmbH, Adelshofen, Germany) activated with electron beam up to 30 kGy output powers.

CONCLUSIONS

The compounding and injection molding of polymer–particle composites made of technical thermoplastic polymers and nickel-based microparticles with filler contents up to 65 vol % were successfully performed in kneading and injection molding process. Torques in kneading process as well as injection molding parameters are significantly influenced by viscosity of the composite melts. The composites show homogeneous distributed microparticles and particle–particle interactions at all examined filler contents, verified by EDX. The examined polymers show residue-free decomposition at temperatures above 550°C using temperature profiles in TGA as well as in debindering test, even for their composites. Thus, the main

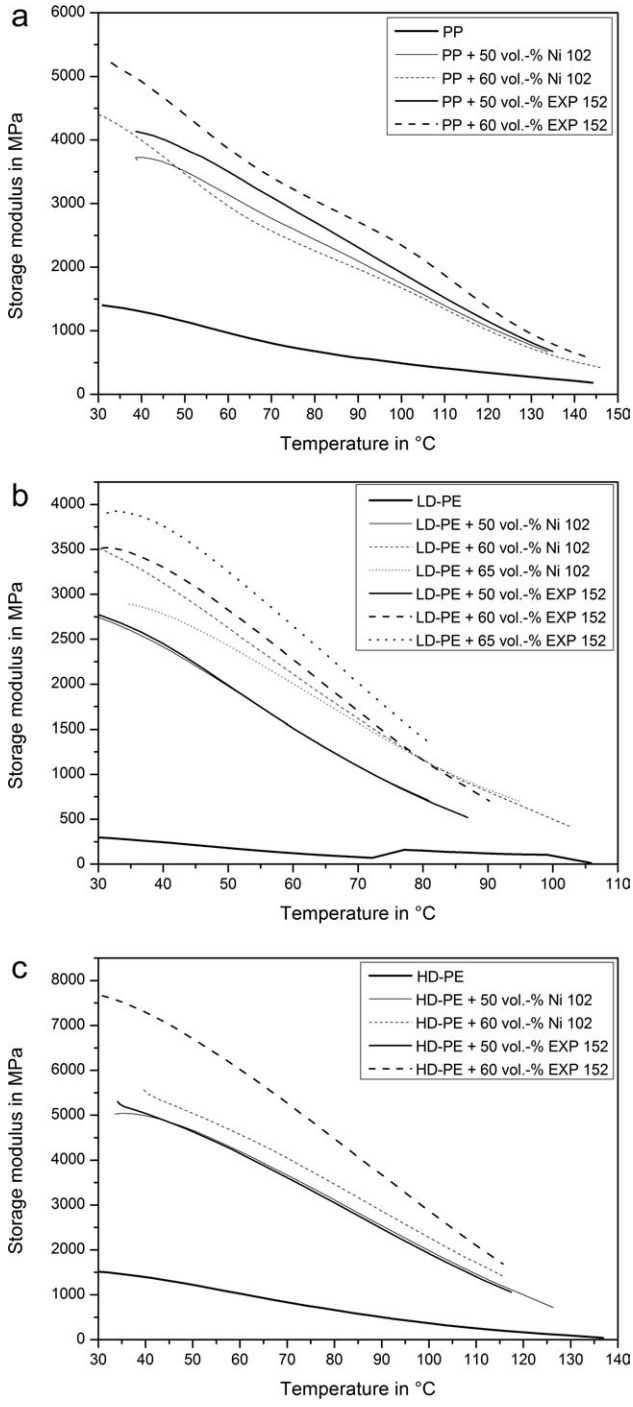

Figure 8. Storage modulus vs. temperature of (a) PP, (b) LD-PE, (c) HD-PE and their polymer–particle composites.

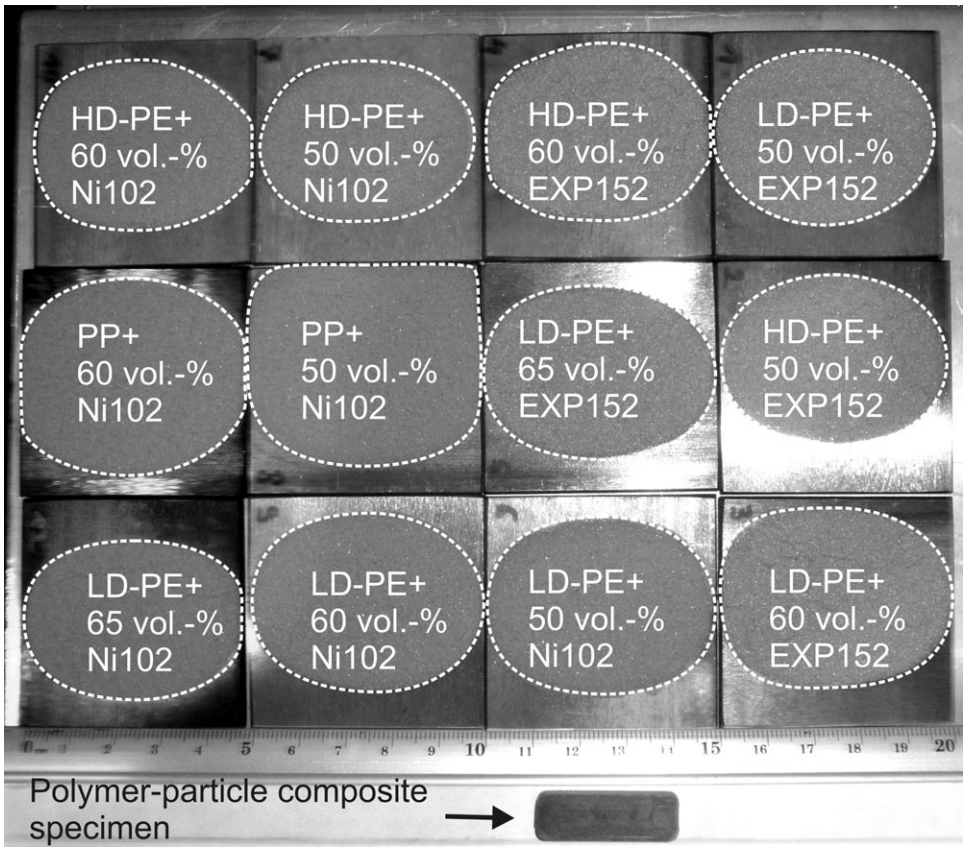

Figure 9. Results of debindering tests on rectangular injection molded polymer–particle composite specimen (30 × 10 × 4 mm^3) at temperature up to 600°C under nitrogen atmosphere.

requirement for application in brazing process can be fulfilled. Adjusted polymer weight percent was analyzed in TGA to prove the desired volume percent of braze metal particles in composites.

Crystallinity of the polymers decreases slightly by adding microparticles. However, filler content of the composites and crystallinity of the polymer matrix cannot be correlated. Undefined cooling after injection molding results in lower crystallinity and equal or lower melt peak temperature of the polymer matrix compared with the prior defined cooling at 5°C/min. Due to the low crystallinity of LD-PE shrinkage of its injection molded composites will be minimized. Storage modulus of polymers was increased up to 15 times by adding microparticles. With increasing temperature, the mechanical reinforcing of the rigid particles in the composites becomes smaller caused by softening of the polymer matrix. HD-PE + 60 vol % EXP 152 shows at 30°C a storage modulus of 7600 MPa, which is up to 1.44 times higher than the PP- and LD-PE composites at equal filler content. Mechanical properties of composites containing EXP 152 particles show improved performance compared to composites containing Ni 102 particles. In summary, LD-PE + 65 vol % EXP 152 exhibits the most suitable material performance for the expected application. However, the flow ability of the polymer matrix has to be further decreased to improve form stability in brazing processes.

ACKNOWLEDGMENTS

The authors would like to thank the Deutsche Forschungsgemeinschaft (DFG) for financial support (Project no. KI 1656/1-1, MO 881/16-1).

REFERENCES

1. Bhattacharya, S. N.; Musa, R. K.; Rahul, K. G. In Polymeric Nanocomposites: Theory and Practice, Carl Hanser Verlag: München, **2007**; Chapter 7, p 339.
2. Cirino, M.; Friedrich, K.; Pipes R. B. *Composites* **1988**, *19*, 383.
3. Yi, X.-S.; Wu, G.; Pan, Y. *Polym. Int.* **1997**, *44*, 117.
4. Ahmad, H.; Tofaz, T.; Oli, M. W. U.; Rahman, M. A.; Miah, M. A. J.; Tauer, K. *Mater. Sci. Appl.* **2010**, *1*, 109.
5. Kirchberg, S.; Rudolph, M.; Ziegmann, G.; Peuker, U. A. *J. Nanomater., Special Issue: Synthesis, Properties, and Applications of Polymeric Nanocomposites* **2012**, Article ID 670531, doi:10.1155/2012/670531, 1–8.
6. Kirchberg, S. Einfluss von Füllgrad und Geometrie weichmagnetischer Partikel auf die Verarbeitungs- und Materialeigenschaften ausgewählter Thermoplaste, PhD Thesis, Papierflieger: Clausthal-Zellerfeld, **2009**.
7. Sarasa, M; Gerling, D.; Kastinger, G.; Schumacher, A. In Joint Czech Polish Conference on project GACR430813,

Low voltage electrical machines, Brünn: Czech Republic, **2004**, p 91.

8. Hussain, F.; Hojjati, M.; Okamoto, M.; Gorga, R. F. J. *J. Compos. Mater.* **2006**, *40*, 1511.
9. Jacobson, D. M.; Humpston, G. In Principles of Brazing, ASM International, **2005**.
10. Lugscheider, E.; Partz, K.-D. *Welding J.* **1983**, *62*, 160.
11. Bach, Fr.-W.; Möhwald, K.; Holländer, U.; Schaup, J.; Roxlau, C.; Langohr, A. *Int. J. Mater. Res. (formerly Z. Metallkd.)* **2011**, *102*, 964.
12. Bach, Fr.-W.; Möhwald, K.; Holländer, U. *Key Eng. Mater.* **2010**, *438*, 73.
13. Feldbauer, S. L. Proceedings of the 3rd Int. Brazing and Soldering Conf., San Antonio, USA, **2006**, 334.
14. American Standard AWS C3.6M/C3.6:2008, Miami, USA, **2008**.
15. Stratton, P. F. Proceedings of the 7th Int. Conf. on Brazing and Diffusion Bonding, Aachen, Germany, **2004**, 181.
16. Kirchberg, S.; Ziegmann, G. *Appl. Rheol.* **2011**, *21*, 35495.
17. Ehrenstein, G. W.; Riedel, G.; Traviel, P. In Praxis der thermischen Analyse von Kunststoffen, Carl Hanser Verlag: München, **1998**; Vol. 2, Chapter 1, p 16.
18. Kirchberg, S.; Ziegmann, G. *J. Compos. Mater.* **2009**, *43*, 1323.